Transition width of the $J^\pi = 1^-$ two-phonon state of ^{88}Sr

D. Savran,[1,*] J. Isaak,[2] K. Albe,[3] A. D. Ayangeakaa,[4,5] M. Beuschlein,[2] S. W. Finch,[5,6] D. Gribble,[4,5] A. Gupta,[2] J. Hauf,[2] X. K.-H. James,[4,5] R. V. F. Janssens,[4,5] S. R. Johnson,[4,5] P. Koseoglou,[2] T. M. Kowalewski,[4,5] B. Löher,[1] O. Papst,[2] N. Pietralla,[2] J. Rohrer,[3] A. Saracino,[4,5] N. Sensharma,[4,5] W. Tornow,[5,6] and V. Werner[2]

[1]*GSI Helmholtzzentrum für Schwerionenforschung GmbH, Darmstadt 64291, Germany*

[2]*Institute for Nuclear Physics, Department of Physics, Technische Universität Darmstadt, Darmstadt 64289, Germany*

[3]*Institut für Materialwissenschaft, Technische Universität Darmstadt, Darmstadt 64287, Germany*

[4]*Department of Physics and Astronomy, University of North Carolina, Chapel Hill 27599-3255, USA*

[5]*Triangle Universities Nuclear Laboratory, Durham, North Carolina 27708, USA*

[6]*Department of Physics, Duke University, Durham, North Carolina 27708-0308, USA*

(Received 22 May 2024; accepted 24 June 2024; published 14 August 2024)

The ground-state decay width of the two-phonon $J^\pi = 1^-$, 4742 keV state of ^{88}Sr has been determined with the relative self-absorption method combined with a monoenergetic photon beam. This width is important to determine the decay transition strengths into the ground state and the one-phonon 2_1^+ and 3_1^- levels which are required to verify the two-phonon character of the $J^\pi = 1^-$ state. The experiment was performed at the High Intensity γ-ray Source (HIγS) using a novel experimental approach to adapt the relative self-absorption method to monoenergetic photon beams. The result for the ground-state decay width is, thus, independent of any calibration standard and confirms the two-phonon character of the ^{88}Sr, $J^\pi = 1^-$, 4742 keV state within an improved uncertainty.

DOI: 10.1103/PhysRevC.110.024312

I. INTRODUCTION

The low-energy excitation spectrum of atomic nuclei near and at closed shells is of central interest in nuclear structure physics, as precise and complete spectroscopy can be achieved experimentally, and an understanding of the basic nature of nuclear excitations can be inferred from comparisons with theoretical models. In particular, low-lying collective vibrations and multiphonon coupled excitations have been used for a long time as building blocks of nuclear structure (see, e.g., Ref. [1] and references therein). Prime examples in even-even nuclei are the low-lying 2^+ and 3^- states described by quadrupole and octupole phonon oscillations of the nuclear surface, with the couplings among these elementary modes of excitation being so-called multiphonon states. While multiphonon states of identical phonons, such as $(2^+ \otimes 2^+)$ or $(3^- \otimes 3^-)$, might suffer from Pauli blocking leading to strong anharmonicities, the quadrupole-octupole two-phonon coupling $(2^+ \otimes 3^-)$ is expected to be characterized by a two-phonon wave function with higher purity.

Recently, the two-phonon nature of the 4742 keV, $J^\pi = 1^-$ member of the $(2^+ \otimes 3^-)$ quintuplet of ^{88}Sr was investigated [2]. The spin and parity quantum numbers 1^- had been clarified in Ref. [3]. A unique fingerprint of its two-phonon character is the $E2$ decay strength of the $1^-_{4742\,\mathrm{keV}} \to 3^-_1$ transition which, within this picture, should equal the $B(E2, 2^+_1 \to 0^+_1)$ transition probability of the one-phonon 2^+_1 level. For this purpose, the decay branchings of the 1^- state were studied with high sensitivity in γ-ray spectroscopy following the β decay of ^{88}Rb [2]. In terms of the partial width Γ, a branching ratio of

$$\frac{\Gamma(1^-_{4742\,\mathrm{keV}} \to 3^-_1)}{\Gamma(1^-_{4742\,\mathrm{keV}} \to 0^+_1)} = 0.0372(29) \tag{1}$$

was determined. Together with the value of $\Gamma_0^2/\Gamma = 107(14)$ meV of Ref. [4] and the $\Gamma_0/\Gamma = 0.811(5)$ ratio derived in Ref. [2], a transition strength of $B(E2, 1^-_{4742\,\mathrm{keV}} \to 3^+_1) = 8.0(12)$ W.u. is calculated. This value is in good agreement, within statistical uncertainties, with the $B(E2, 2^+_1 \to 0^+_1) = 7.6(4)$ W.u. probability for the ground-state transition. The uncertainty in the $B(E2, 1^-_{4742\,\mathrm{keV}} \to 3^-_1)$ value is dominated by that of the Γ_0^2/Γ ratio [4], which is about 13%. Hence, a more precise measurement of the ground-state decay width Γ_0 is required to further improve the precision of the decay properties of the 1^-, 4742 keV state and to herewith provide a more stringent test of its two-phonon character. Relative self-absorption (RSA) is a powerful method to derive the Γ_0 value directly in a model-independent way [5,6]. The results of its application are presented below.

This article is organized as follows: in the next section, the experiment is presented together with the RSA method and the corresponding data analysis. The results are then discussed in Sec. III, followed by a concluding paragraph.

II. EXPERIMENT AND ANALYSIS

The experiment was carried out at the Triangle University Nuclear Laboratory (TUNL) using the High Intensity

*Contact author: d.savran@gsi.de

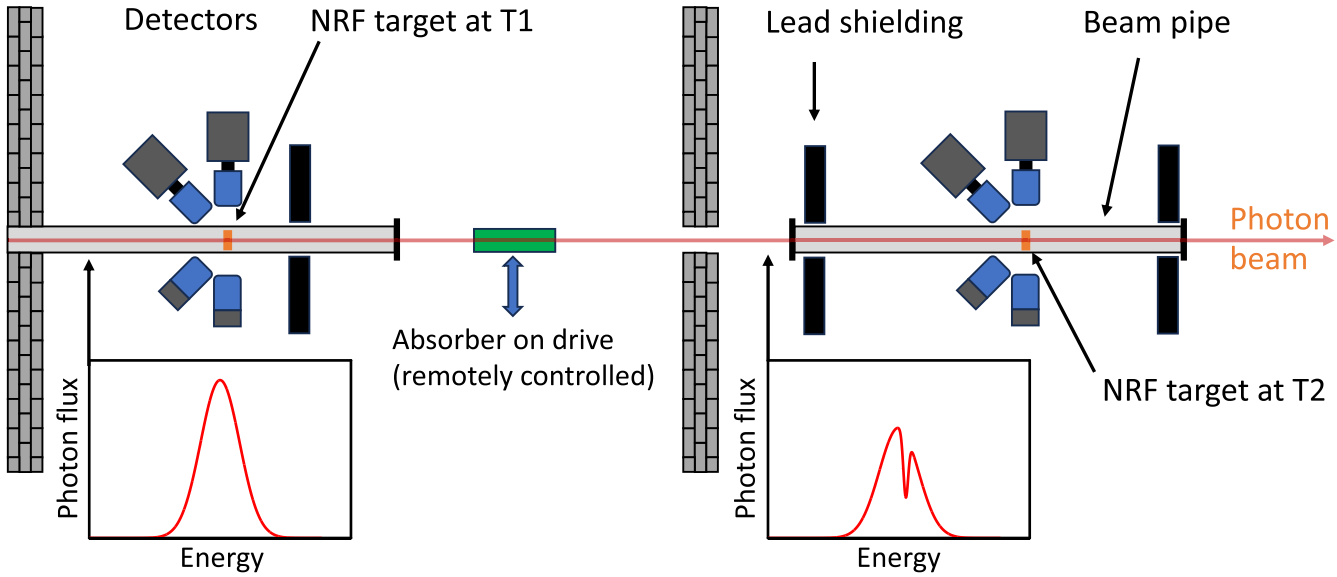

FIG. 1. Schematic drawing of the experimental setup. The two NRF target stations are placed in separate, well-shielded experimental areas. As shown schematically in the figure, the beam line was evacuated in the vicinity of the setups in order to reduce background from small-angle scattering on air. The absorption target was not positioned in the vacuum. It was mounted on a linear drive enabling motion as described in the text. The two beam profiles indicate the effect of self-absorption within the absorber.

γ-ray Source (HIγS) [7]. The experimental setup, illustrated schematically in Fig. 1, follows the concept presented in Ref. [8], which combines the RSA method with the usage of a monoenergetic photon beam. The two γ-ray spectrometers available at TUNL were employed: the clover array [9] and the γ^3 setup [10]. These are labeled T1 and T2 in Fig. 1, respectively. They were installed, one behind the other, along the HIγS beam line in the facility's two experimental areas. With this approach, two nuclear resonance fluorescence (NRF) [11] experiments were performed simultaneously at positions T1 and T2: one before and one after the beam passed through the absorption target (absorber). With the two setups being in separate areas, and with additional lead shielding being placed in critical locations (see Fig. 1), both spectrometers were well shielded from the absorber and from each other. Measurements without scattering targets at T1 and T2 were performed to study and characterize the background conditions [12]. The absorber was placed on a remotely controlled linear drive in order to facilitate switching between configurations with and without absorption target during the experiment.

For both NRF setups, a combination of high-purity germanium (HPGe) and LaBr detectors was used. Table I provides information on the detectors at both target positions, together with the corresponding target parameters. The NRF targets were composed of $SrCO_3$, enriched to 99.915% in ^{88}Sr. Since the natural abundance of ^{88}Sr is 82.58% and the self-absorption effect is not disturbed by the presence of other Sr isotopes in the compound, the absorber consisted of natural $SrCO_3$ with a total mass of 204.7 g. It was cylindrical in shape with a diameter of 30 mm, sufficient to ensure that the complete beam passed through it before impinging on NRF target T2. Measurements with and without the absorber in the beam could be carried out without interrupting the photon beam. About three hours of data with and one hour without absorber were accumulated at a mean photon-beam energy of 4.74 MeV.

As discussed in Ref. [8], the basic principle of the self-absorption technique consists of investigating the absorption spectrum itself rather than determining the NRF cross section by counting the number of emitted photons following the excitation of the nucleus by the photon beam. For a given level, the associated absorption line is directly related to the excitation cross section and the ground-state decay width Γ_0. However, since the width of an excited state is usually in the meV to eV range, the width of the corresponding absorption line will be of this order as well and, as a result, the properties of the absorption line cannot be measured directly with high-efficient, state-of-the-art γ-ray detectors as their intrinsic resolution is insufficient. To overcome this difficulty, in the present work, the NRF reaction rate on the same isotope is utilized as a measure for the absorption cross section by

TABLE I. Target parameters and list of all HPGe and LaBr detectors included in the NRF setups at T1 and T2. The position is given by (θ, ϕ) with the polar angle θ and the azimuthal angle ϕ (in degrees) with respect to the horizontally polarized incident photon beam.

		T1	T2
detectors	HPGe	(90,0), (90,90)[a]	(90,0), (90,90)
		(135,0), (125,135)	(135,0), (125,135)[a]
	LaBr	(90,180), (90,270)	(90,180), (90,270)
		(135,218), (135,321)[a]	(135,218), (135,321)
target	mass	2.471 g	4.250 g
	diameter	20 mm	25 mm

[a]Not operational during the present experiment.

comparing the number of reactions at T2 with and without the absorber inserted in the photon beam. The change in reaction rate between these two settings is directly related to the NRF absorption cross section. The effect of the absorber on the energy distribution of the photon beam is sketched schematically in Fig. 1. In addition to the overall reduction in intensity due to atomic processes, a characteristic absorption line is imprinted on the photon-beam distribution by the NRF reaction.

In principle, with the present setup, both NRF experiments can be performed simultaneously as outlined in Ref. [8]. However, in order to reduce systematic uncertainties, two sets of experiments were carried out, one with, and another without, absorber in the photon beam between T1 and T2. As presented in [8], the self-absorption factor R is given by

$$R = 1 - \frac{N_{\mathrm{T2}}}{N_{\mathrm{T1}} \times f}, \tag{2}$$

with N_{T1} and N_{T2} being the number of NRF reactions observed at T1 and T2, respectively. The normalization factor f is defined by

$$f = \frac{M^{\mathrm{T2}}}{M^{\mathrm{T1}}} \times \frac{\epsilon_\gamma^{\mathrm{T2}}(4742\ \mathrm{keV})}{\epsilon_\gamma^{\mathrm{T1}}(4742\ \mathrm{keV})} \times \frac{\tau_{\mathrm{live}}^{\mathrm{T2}}}{\tau_{\mathrm{live}}^{\mathrm{T1}}} \times \frac{N_\gamma^{\mathrm{T2}}}{N_\gamma^{\mathrm{T1}}}, \tag{3}$$

where $M, \epsilon_\gamma, \tau_{\mathrm{live}}, N_\gamma$ are the target mass, the γ-ray detection efficiency at $E_\gamma = 4742$ keV, the detector live time, and the integrated photon flux at target positions T1 and T2, respectively. As shown in Refs. [13,14], the low-energy part of the measured γ-ray spectrum and, in particular, the intensity in the 511 keV annihilation peak are proportional to the integrated photon flux impinging on the target. More precisely, at a given energy, the number of counts in this 511 keV peak (N_{511}) is proportional to the product of integrated photon flux, target mass, detection efficiency and effective live time

$$N_{511} \propto N_\gamma \times M \times \epsilon_\gamma(511\ \mathrm{keV}) \times \tau_{\mathrm{live}}. \tag{4}$$

With Eqs. (3) and (4) the factor f can be rewritten as

$$f = \frac{N_{511}^{\mathrm{T2}}}{N_{511}^{\mathrm{T1}}} \times \frac{\epsilon_\gamma^{\mathrm{T1}}(511\ \mathrm{keV})}{\epsilon_\gamma^{\mathrm{T2}}(511\ \mathrm{keV})} \times \frac{\epsilon_\gamma^{\mathrm{T2}}(4742\ \mathrm{keV})}{\epsilon_\gamma^{\mathrm{T1}}(4742\ \mathrm{keV})}, \tag{5}$$

which requires the knowledge of the efficiency ratio at $E_\gamma = 511$ keV and $E_\gamma = 4742$ keV for the setups at T1 and T2. For the measurement without absorber, obviously $R = 0$ and Eq. (2) reduces to

$$\frac{\bar{N}_{\mathrm{T2}}}{\bar{N}_{\mathrm{T1}} \times \bar{f}} = 1, \tag{6}$$

with the factor $\bar{f}$ being equivalent to Eq. (5) using the corresponding count rates $\bar{N}_{511}$. The ratio of Eq. (2) and Eq. (6) leads to a simplification of the determination of the absorption factor R as

$$\begin{aligned} R &= 1 - \frac{N_{\mathrm{T2}}}{N_{\mathrm{T1}} \times f} \times \frac{\bar{N}_{\mathrm{T1}} \times \bar{f}}{\bar{N}_{\mathrm{T2}}} \\ &= 1 - \frac{N_{\mathrm{T2}}}{N_{\mathrm{T1}}} \times \frac{\bar{N}_{\mathrm{T1}}}{\bar{N}_{\mathrm{T2}}} \times \frac{N_{511}^{\mathrm{T1}}}{N_{511}^{\mathrm{T2}}} \times \frac{\bar{N}_{511}^{\mathrm{T2}}}{\bar{N}_{511}^{\mathrm{T1}}}, \end{aligned} \tag{7}$$

which requires only the count rates in the NRF reaction and in the 511 keV peak at T1 and T2 from measurements with and without absorber, respectively. This procedure strongly reduces systematic uncertainties in the determination of R and, thus, in the extraction of the Γ_0 width.

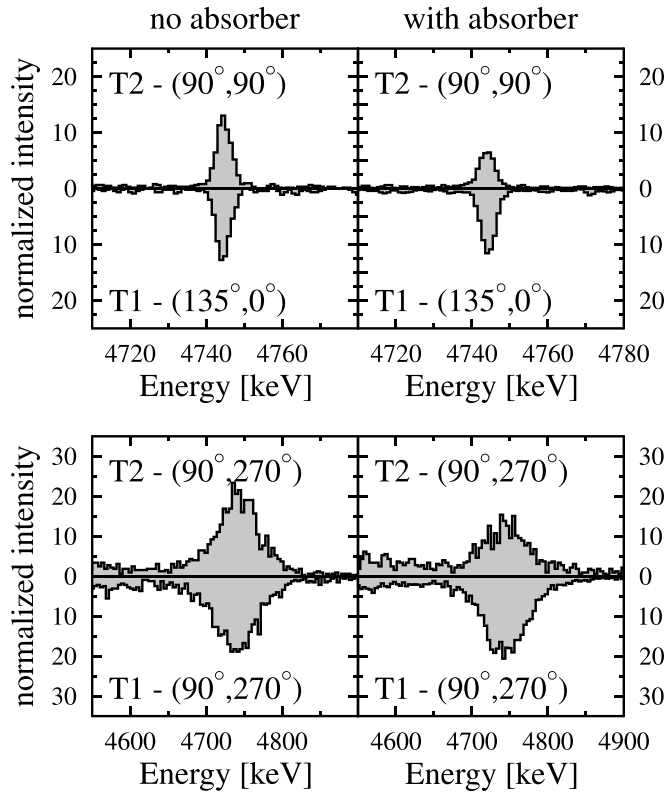

FIG. 2. Measured spectra of a HPGe detector (upper row) and a LaBr scintillator (lower row) at both target positions for runs with (right) and without (left) absorber. Each spectrum was normalized to the intensity of the 511 keV peak in the same spectrum.

Figure 2 provides examples of HPGe and LaBr spectra in the energy region of the 4742 keV γ ray corresponding to the $1^-_{4742} \rightarrow 0^+_1$ transition. These were measured at the T1 and T2 positions with and without absorber and were properly normalized to the intensity of their respective 511 keV lines. It is obvious that the peak for the detectors at T2 is suppressed in the measurement with absorber, herewith illustrating the impact of nuclear self-absorption.

For the determination of the γ-ray intensities in the HPGe spectra, the required peak areas were extracted with the usual procedure of subtracting the background underneath a peak of interest using a linear fit to the regions left and right of it. Due to the high energy resolution of the HPGe detectors, this procedure is well suited and, with Eq. (7), a value of $R = 0.445(56)$ is derived for the self-absorption factor.

A different procedure was applied to the LaBr spectra in order to accommodate the reduced energy resolution of the scintillators. Rather than focusing solely on the full-energy peak, spectra covering the 4000–5000 keV region were considered. The analysis took into account the detector's response as well as various background contributions. In a first step, the γ-ray background stemming from cosmic radiation was modeled. The energy dependence of this contribution was obtained from long-duration measurements without any photon

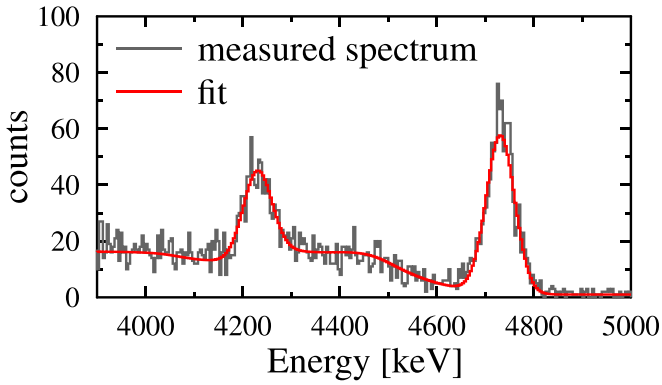

FIG. 3. Measured spectrum and fit of the LaBr detector at $(\theta, \phi) = (90°, 270°)$. The data were measured at the T2 location without the absorber in place.

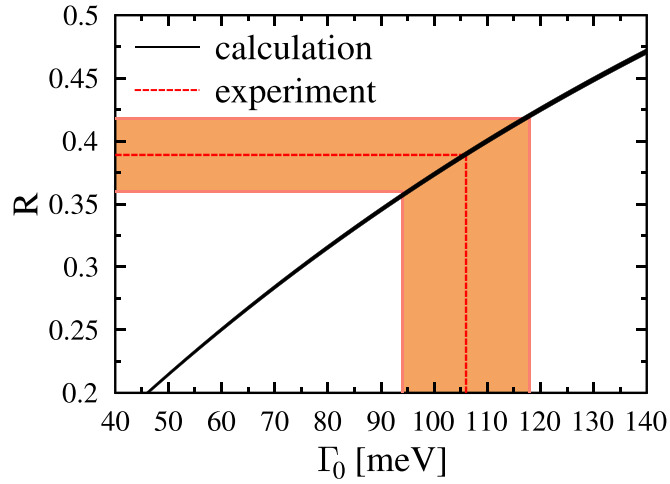

FIG. 4. Calculated correlation between the self-absorption factor R and the ground-state decay width Γ_0 (black solid line). The width of the line follows from the uncertainty in T_{eff}. The orange band around the experimental value corresponds to the uncertainty in R and the corresponding projected error in Γ_0.

beam. It exhibited a linear dependence over a large energy region above 3 MeV. It was scaled to the spectra with beam using the region above the 4742 keV full-energy peak. The background contribution induced by the photon beam itself was obtained from measurements at a mean beam energy of 4.44 MeV without scattering targets in the T1 and T2 locations; see Ref. [12]. Its energy dependence is described well by a square-root model. Finally, the LaBr detector response for 4742 keV γ rays was simulated using the GEANT4 package [15,16], and was folded with a Gaussian function to take the energy resolution into account. It was fitted to the measured spectra with a normalization factor and the width of the Gaussian as free parameters in the fitting procedure. In addition to the response function, the contribution from the beam background was added with a square-root dependence of $N_{\text{BG}} = A \times \sqrt{E_0 - E}$ with A and E_0 being free parameters. An example of a LaBr spectrum with the resulting fit is found in Fig. 3. All the LaBr spectra were analysed with this procedure to extract the corresponding peak intensities.

From the analysis of the γ-ray intensities, measured by the LaBr detectors, a self-absorption factor of $R = 0.370(33)$ was determined. Although somewhat smaller, this R value agrees within statistical uncertainties with that reported above from the spectra measured by the HPGe detectors. Averaging both results leads to the final value of $R = 0.389(29)$ for the self-absorption factor.

III. RESULTS AND DISCUSSION

Figure 4 presents the calculated relation between the self-absorption R and the ground-state decay width Γ_0. For this calculation, the Doppler broadening due to the thermal motion of the nuclei was taken into account. This was handled in terms of an effective temperature T_{eff} [11,17–19]. For the present case of Sr_2CO_3, T_{eff} was estimated in an approach analogous to that employed recently in Ref. [6]. It starts from the phonon density of states (phDOS) obtained from density functional theory (DFT) calculations as implemented in the GEANT4 code [20] in conjunction with the PHONOPY package [21]. A plane-wave cutoff of 1200 eV and a k-point density of 2 Å were used. The T_{eff} value was computed both in the local density approximation (LDA) [22] and in the PBE flavour of the generalized gradient approximation [23]. For a thermodynamical temperature of 295 K, the resulting average between the two computations of $T_{\text{eff}} = 340(5)$ K was then adopted to derive the relation between R and Γ_0 displayed in Fig. 4.

A value of $\Gamma_0 = 106(12)$ meV is extracted from the correlation with the self-absorption value $R = 0.389(29)$ (Fig. 4). This value is lower than the literature ones of $\Gamma_0 = 117(25)$ meV and 132(17) meV determined from the NRF experiments reported, respectively, in Refs. [24] and [4] using the ratio $\Gamma_0/\Gamma = 0.811(5)$ of Ref. [2]. Nevertheless, all three decay widths agree within their respective uncertainties. Since they were obtained from independent measurements, the results can be combined in a weighted averaged value of $\Gamma_0 = 115(9)$ meV, i.e., in a decay width of ≈8% precision, which compares favorably with the 13% uncertainty quoted in Ref. [2]. Hence, the present work results in a more precise transition probability of $B(E2, 1^-_{4742\,\text{keV}} \to 3^+_-) = 7.0(8)$ W.u., which translates in an updated value for a probability ratio of

$$\frac{B(E2, 1^-_{4742\,\text{keV}} \to 3^-_1)}{B(E2, 2^+_1 \to 0^+_1)} = 0.92(12). \tag{8}$$

The close agreement with unity is noteworthy as it provides a new, more stringent confirmation of the quadrupole-octupole coupled two-phonon character of the 1^-, 4742 keV state of ^{88}Sr.

IV. CONCLUSIONS

The ground state decay width of the $J^\pi = 1^-$, 4742 keV state of ^{88}Sr has been measured using the nuclear self-absorption method. A new combination of two NRF setups at the HIγS facility was used. It enables RSA experiments to be performed with a quasimonoenergetic photon beam, herewith greatly reducing systematic uncertainties. The resulting

$\Gamma_0 = 106(11)$ meV width yields a new, more accurate strength for the 1^- level decay into the 3_1^- state. The values of the two transition probabilities $B(E2, 1^-_{4742\,\mathrm{keV}} \to 3^+_-) = 7.0(8)$ W.u. and $B(E2, 2^+_1 \to 0^+_1) = 7.6(4)$ W.u. are in good agreement and, thus, confirm the two-phonon character of the 1^- state.

The measurements reported in the present work required only about 4 hours of beam time, which demonstrates the power and efficiency of the RSA method. This approach enables the extraction of level widths without the need for any reaction model, and its combination with a quasimonoenergetic photon beam is, therefore, ideally suited for high-precision measurements aiming at investigating specific nuclear excitations such as those presented here.

ACKNOWLEDGMENTS

The authors thank the HIγS accelerator staff for providing excellent photon beams and experimental conditions as well as the GSI target laboratory for preparing the precisely manufactured NRF targets. This work is supported by the Deutsche Forschungsgemeinschaft (DFG, German Research Foundation), Project-ID 499256822–GRK 2891 "Nuclear Photonics," by the grant "Nukleare Photonik" within the LOEWE program [LOEWE/2/11/519/03/04.001(0008)/62] and the Research Cluster ELEMENTS (Project ID 500/10.006) of the State of Hesse, and by the U.S. Department of Energy, Office of Nuclear Physics under Grants No. DE-FG02-97ER41033 (TUNL), No. DE-FG02-97ER41041 (UNC), and No. DE-SC0023010 (UNC).

[1] R. F. Casten, *Nuclear Structure from a Simple Perspective*, 2nd ed. (Oxford University Press, New York, 1990).
[2] J. Isaak, D. Savran, N. Pietralla, N. Tsoneva, A. Zilges, K. Eberhardt, C. Geppert, C. Gorges, H. Lenske, and D. Renisch, Phys. Rev. C **108**, L051301 (2023).
[3] N. Pietralla, V. N. Litvinenko, S. Hartman, F. F. Mikhailov, I. V. Pinayev, G. Swift, M. W. Ahmed, J. H. Kelley, S. O. Nelson, R. Prior, K. Sabourov, A. P. Tonchev, and H. R. Weller, Phys. Rev. C **65**, 047305 (2002); **65**, 069901(E) (2002).
[4] L. Käubler, H. Schnare, R. Schwengner, H. Prade, F. Dönau, P. von Brentano, J. Eberth, J. Enders, A. Fitzler, C. Fransen, M. Grinberg, R.-D. Herzberg, H. Kaiser, P. von Neumann-Cosel, N. Pietralla, A. Richter, G. Rusev, C. Stoyanov, and I. Wiedenhöver, Phys. Rev. C **70**, 064307 (2004).
[5] C. Romig, D. Savran, J. Beller, J. Birkhan, A. Endres, M. Fritzsche, J. Glorius, J. Isaak, N. Pietralla, M. Scheck, L. Schnorrenberger, K. Sonnabend, and M. Zweidinger, Phys. Lett. B **744**, 369 (2015).
[6] U. Friman-Gayer, C. Romig, T. Hüther, K. Albe, S. Bacca, T. Beck, M. Berger, J. Birkhan, K. Hebeler, O. J. Hernandez, J. Isaak, S. König, N. Pietralla, P. C. Ries, J. Rohrer, R. Roth, D. Savran, M. Scheck, A. Schwenk, R. Seutin, and V. Werner, Phys. Rev. Lett. **126**, 102501 (2021).
[7] H. R. Weller, M. W. Ahmed, H. Gao, W. Tornow, Y. K. Wu, M. Gai, and R. Miskimen, Prog. Part. Nucl. Phys. **62**, 257 (2009).
[8] D. Savran and J. Isaak, Nucl. Instrum. Methods Phys. Res. A **899**, 28 (2018).
[9] A. D. Ayangeakaa, U. Friman-Gayer, and R. V. F. Janssens, Innovation News Network, https://www.innovationnewsnetwork.com/nuclear-structure/10491/.
[10] B. Löher, V. Derya, T. Aumann, J. Beller, N. Cooper, M. Duchene, J. Endres, E. Fiori, J. Isaak, J. Kelley, M. Knörzer, N. Pietralla, C. Romig, D. Savran, M. Scheck, H. Scheit, J. Silva, A. P. Tonchev, W. Tornow, H. Weller, V. Werner, and A. Zilges, Nucl. Instrum. Methods Phys. Res. A **723**, 136 (2013).
[11] A. Zilges, D. Balabanski, J. Isaak, and N. Pietralla, Prog. Part. Nucl. Phys. **122**, 103903 (2022).
[12] D. Savran, J. Isaak, A. D. Ayangeakaa, M. Beuschlein, S. W. Finch, D. Gribble, A. Gupta, J. Hauf, X. K. James, R. V. F. Janssens, S. R. Johnson, P. Koseoglou, T. Kowalewski, B. Löher, O. Papst, N. Pietralla, A. Saracino, N. Sensharma, W. Tornow, and V. Werner, Nuovo Cimento C **47**, 57 (2024).
[13] M. Tamkas, E. Açıksöz, J. Isaak, T. Beck, N. Benouaret, M. Bhike, I. Boztosun, A. Durusoy, U. Gayer, Krishichayan, B. Löher, N. Pietralla, D. Savran, W. Tornow, V. Werner, A. Zilges, and M. Zweidinger, Nucl. Phys. **987**, 79 (2019).
[14] D. Savran, J. Isaak, R. Schwengner, R. Massarczyk, M. Scheck, W. Tornow, G. Battaglia, T. Beck, S. W. Finch, C. Fransen, U. Friman-Gayer, R. Gonzalez, E. Hoemann, R. V. F. Janssens, S. R. Johnson, M. D. Jones, J. Kleemann, Krishichayan, D. R. Little, D. O'Donnell *et al.*, Phys. Rev. C **106**, 044324 (2022).
[15] S. Agostinelli, J. Allison, K. Amako, J. Apostolakis, H. Araujo, P. Arce, M. Asai, D. Axen, S. Banerjee, G. Barrand, F. Behner, L. Bellagamba, J. Boudreau *et al.*, Nucl. Instrum. Methods Phys. Res. A **506**, 250 (2003).
[16] J. Allison, K. Amako, J. Apostolakis, H. Araujo, P. Arce Dubois, M. Asai, G. Barrand, R. Capra, S. Chauvie, R. Chytracek, G. A. P. Cirrone, G. Cooperman, G. Cosmo, G. Cuttone, G. G. Daquino, M. Donszelmann, M. Dressel, G. Folger, F. Foppiano, J. Generowicz *et al.*, IEEE Trans. Nucl. Sci. **53**, 270 (2006).
[17] F. R. Metzger, Prog. Nucl. Phys. **7**, 53 (1959).
[18] W. E. Lamb, Phys. Rev. **55**, 190 (1939).
[19] N. Pietralla, P. von Brentano, R.-D. Herzberg, U. Kneissl, J. Margraf, H. Maser, H. H. Pitz, and A. Zilges, Phys. Rev. C **52**, R2317 (1995).
[20] J. J. Mortensen, A. H. Larsen, M. Kuisma, A. V. Ivanov, A. Taghizadeh, A. Peterson, A. Haldar, A. O. Dohn, C. Schäfer, E. O. Jonsson, E. D. Hermes, F. A. Nilsson, G. Kastlunger, G. Levi, H. Jonsson, H. Häkkinen, J. Fojt, J. Kangsabanik, J. Sodequist, J. Lehtomäki *et al.*, J. Chem. Phys. **160**, 092503 (2024).
[21] A. Togo, J. Phys. Soc. Jpn. **92**, 012001 (2023).
[22] J. P. Perdew and Y. Wang, Phys. Rev. B **45**, 13244 (1992).
[23] J. P. Perdew, K. Burke, and M. Ernzerhof, Phys. Rev. Lett. **77**, 3865 (1996).
[24] F. R. Metzger, Phys. Rev. C **11**, 2085 (1975).